

Experimental and numerical study of shear crack propagation in concrete specimens

Hadi Haeri^{*1}, Vahab Sarfarazi² and Alireza Bagher Shemirani^{3,4}

¹Young Researchers and Elite Club, Bafgh Branch, Islamic Azad University, Bafgh, Iran

²Department of Mining Engineering, Hamedan University of Technology, Hamedan, Iran

³Department of Civil Engineering, SADRA Institute of Higher Education, Tehran, Iran

⁴Department of Civil Engineering, Sharif University of Technology, Tehran, Iran

(Received January 15, 2017, Revised March 16, 2017, Accepted May 21, 2017)

Abstract. A coupled experimental-numerical study on shear fracture in concrete specimens with different geometries is carried out. The crack initiation, propagation and final breakage of concrete specimens are experimentally studied under compression loading. The load-strain and the strength of the specimens are experimentally measured, indicating decreasing effects of the shear behavior on the failure load of the specimen. The effects of specimen geometries on the shear fracturing path in the concrete specimens are also investigated. Numerical models using an indirect boundary element method are made to evaluate the crack propagation paths of concrete specimens. These numerical results are compared with the performed experiments and are validated experimentally.

Keywords: shear behavior; concrete specimens; crack propagation; load-strain analysis

1. Introduction

Concrete is one of the most widely used construction material. It has good compressive strength, durability, fire resistance and can be cast to fit any structural shape. Shear failure of concrete is a common mode of failure in civil engineering infrastructure. Therefore, the shear fracturing behavior of concrete under mixed mode loading needs to be studied in structural members made of concrete. Shear failure in concrete has been studied extensively due to the complexity of shear fracturing behavior. Similar to other types of brittle materials like rocks, failure of concrete specimens subjected to compression typically involves initiation of tensile (wing) cracks. Because shear fractures are primarily observed in brittle materials, better understanding of the shear behavior of concrete and limiting the occurrence of shear cracks may result in development of more ductile concrete (ACI 2008a). There are different types of specimen geometries and testing procedures which can be used to study shear behavior under different loading conditions (Mirsayah and Banthia 2002, ASTM 2002, Fortino and Bilotta 2004, Barragán *et al.* 2006, Deokar and Wakchaure 2011, Sarfarazi *et al.* 2016, Haeri 2015, Haeri and Sarfarazi 2016a, 2016b, 2016c, Haeri *et al.* 2016d). The tests of Brazilian discs and four bending beam specimens are mostly used to determine the shear strength of concrete (Ayatollahi and Aliha 2008, Wang 2010, Dai *et al.* 2010, Dai *et al.* 2011, Ayatollahi and Sistaninia 2011, Yang *et al.* 2011, Zhang and Wong 2012, Zhang and Wong 2013, Ning *et al.*

2015, Weihua *et al.* 2015, Yang 2015, Gerges *et al.* 2015, Panaghi *et al.* 2015, Zhao 2015, Xiang *et al.* 2015, Tang 2015, Haeri and Sarfarazi 2016a, Sarfarazi *et al.* 2016b, Sardemir 2016).

Kaplan (1961) investigated notched concrete beams using linear elastic fracture mechanics (LEFM) under three- and four-point bending configuration in both concrete and rock materials. Based on non-linear fracture mechanics theory, different models for predicting the fracture behavior of concrete are proposed. Examples of such modes are: (a) the Fictitious Crack Model (FC-Model) (Hillerborg 1980); (b) the Crack Band Model (Bazant and Oh 1983, Chuang and Mai 1998); and (c) the Two Parameter Model (Jenq and Shah 1985).

Ozcebe *et al.* (2011) developed a methodological approach to study the breakage of T-shape beams and similarly Ruiz and Carmona (2006) studied the effect of the shape of the crack propagation on rectangular and T-shape beams. Ruiz *et al.* (2006b) theoretically analyzed the crack initiation and propagation in the head of the beam. Savilahti *et al.* (1990) carried out direct shear tests on specimens of jointed plaster material containing non-overlapped and overlapped joints. Wong *et al.* (2001) conducted direct shear tests on specimens made of plaster and natural rocks containing open non-persistent joints to investigate the shear strength and breakage. According to their findings, breakage patterns of the specimens are mainly occurred due to joint separation and affected the shear strength of the specimen. Also, Gehle and Kutter (2003) studied the breakage and shear behavior of intermittent rock joints under direct shear loading conditions. The shear resistance of pre-cracked rock specimens was found to be controlled by the crack inclination.

Many experimental and theoretical studies have also

*Corresponding author

E-mail: haerihadi@gmail.com or h.haeri@bafgh-iau.ac.ir

Table 1 Mix design and mechanical properties of the concrete specimens

| Ingredients ratio (%) | | | Mechanical properties | | | |
|-----------------------|-----------|-------|-----------------------|--------------------------------------------|-----------------------------|-----------------|
| PPC | Fine sand | water | UCS (MPa) | Fracture toughness (MPa m ^{1/2}) | Modulus of elasticity (GPa) | Poisson's ratio |
| 44.5 | 22.5 | 33 | 28 | 0.3 | 17 | 0.21 |

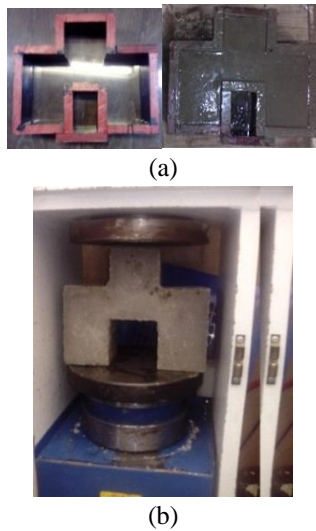


Fig. 1 The process of specimen preparation and laboratory test: (a) A typical mold for concrete-like specimens (b) Experimental set up for concrete specimens simulating the shear action using uniaxial compression

been devoted to study the shear behavior in concrete specimens under mixed mode loading (Wu *et al.* 2006, Sun and Kuchma 2007, Munikrishna 2008, Yang *et al.* 2011).

In this study, the shear fracturing behavior of concrete specimens is investigated experimentally using specially made specimens (using a proper mixture of PPC, fine sands and water). All specimens are tested to failure by subjecting the specimen to uniaxial compression to study the shear behavior of specially made concrete specimens. Using a modified high order displacement discontinuity code, numerical simulations of concrete specimens and fracturing patterns are conducted as well. This modified code uses a cubic variation of displacement discontinuities along each boundary element containing four equal sub-elements. The Linear Elastic Fracture Mechanics (LEFM) theory (by computing the Mode I and Mode II stress intensity factors (SIFs)) and σ -criterion have been implemented in the modified code to predict the crack initiation and propagation paths. Results of the numerical analysis are then compared with experiments, indicating a great agreement between the two methods. Using the experimental results, the numerical simulations are validated and the accuracy and effectiveness of the proposed study of the concrete breaking process under different loading conditions is confirmed.

2. Experimental studies

In this study, concrete specimens with different

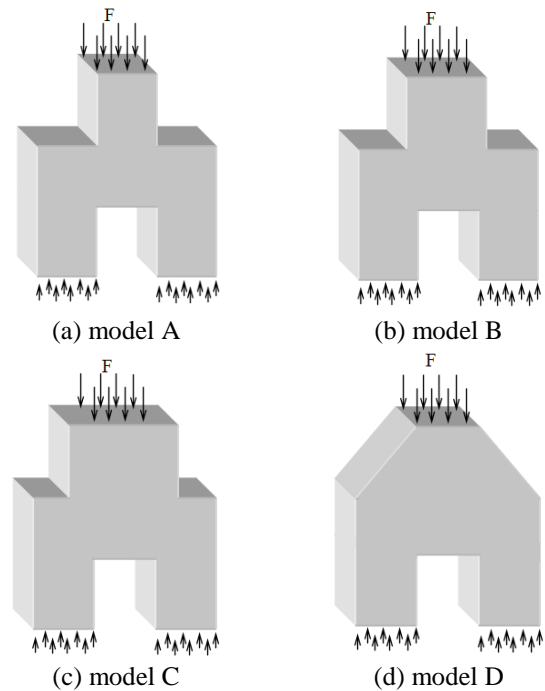


Fig. 2 concrete specimens showing different model geometries for numerical simulation of shearing failure in concrete

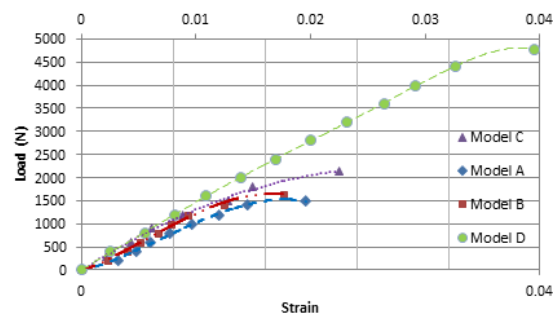


Fig. 3 Load-strain curve for concrete specimens with different geometric models (a) model A (b) model B; (c) model C; (d) model D

geometries are subjected to compression to investigate the mechanisms resulting in initiation and propagation of shear fractures in the specimens. Such tests provide mixed mode I/II conditions resulting in the shear failure of specimens. The following section describes the specimen preparation procedure and the experimental setup.

2.1 Concrete specimen preparation and its mechanical properties

The specimens of quasi-brittle materials (like concrete) with different geometries A mixture of Portland Pozzolana cement (PPC), fine sands and water is commonly used as a quasi-brittle material and a good synthetic material with similar behavior to concrete. Table 1 gives the ingredient ratios (%) and mechanical properties of the prepared intact concrete like specimens tested in the laboratory. The materials tested at this stage were intact with no cracks/fractures.

Table 2 Wing crack initiation loads and the final breakage load for four models, A, B, C, D

| Specimen type | Wing crack initiation load (N) | Failure load (N) |
|---------------|--------------------------------|------------------|
| Model A | 800 | 1500 |
| Model B | 1010 | 1650 |
| Model C | 1600 | 2140 |
| Model D | 2500 | 4780 |

In the laboratory, various types of the specially prepared specimens were tested to study the shear behavior and crack propagation mechanisms. A mold made of wood as shown in Fig. 1(a) was used to make the concrete like specimens. A mixture of PPC, fine sand and water was poured in the mold as shown in Fig. 1(a). The mold is then removed and the specimen is cured for testing after 28 days. Similar specimens but different geometries were prepared and tested using the uniaxial compression machine shown in Fig. 1(b) to subject the specimens into shear failure. The compressive load was applied at a constant loading rate of 0.5 MPa/s during the tests.

3. load-strain analysis of concrete specimens

The load-strain analysis of the specimens with different geometries is of paramount important to study of the shear behavior.

Fig. 3 shows the load-strain curves for four specimen models, A, B, C, and D. The wing cracks were observed at the load levels of 800-2500 N and continued to grow until the failure point in the specimens. The final failure loads of the four models are tabulated in Table 2. As shown in the Table 3, the loads of the specimens at different stages of crack propagation process are increasing for models A to D, respectively. The lowest value of load is for the case A.

Four specimen geometries were studied and are shown in Fig. 2.

4. Shear fracturing behavior of concrete specimens

Shear experiments were carried out on the concrete specimens with the application of the compression load to study the crack initiation, propagation, and fracturing behavior of concrete specimens.

In these experimental shear tests, the tensile cracks are immediately initiated (Fig. 4). The development of wing cracks may be the main cause of the breakage paths in these concrete specimens.

In the model A (Fig. 4(a)), the tensile cracks initiate at the tip of the edges (T1, T2, T3 and T4) and propagate in a straight path and then the specimen failed due to two breakage paths of the propagating cracks from the tips of upper/and lower edges in two specimen sides.

In both models B and C (Fig. 4(b) and 4(c)), the tensile cracks were initiated at the four edges and propagated in a curved path and then the specimen failed due to two breakage paths of the propagating cracks from the upper/and lower edges in two specimen sides.

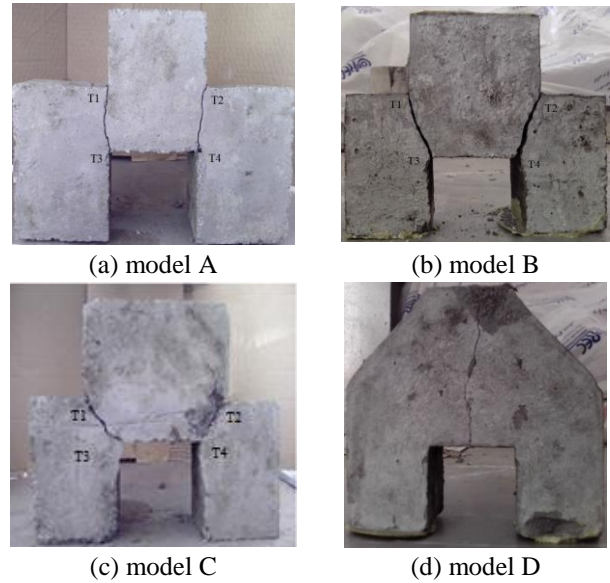


Fig. 4 fracture patterns in concrete specimens with different geometry models

In contrast to above cases, in model D (Fig. 4(d)), the tensile cracks were not propagated from the edges but propagated in a direction (approximately) vertical to the direction of compressive line load. The specimen failed due to the indirect tensile effect (axial splitting) like the cubic specimen in a conventional uniaxial compression test.

5. Numerical simulation of fracturing patterns in concrete specimens

The displacement discontinuity method (DDM) as a boundary element method (BEM) is used for numerical simulation of fractures in the concrete specimens. The code employs a higher order displacement discontinuities variation along each boundary elements in a two dimensional elastostatic body (Crouch 1976a, Crouch and Starfield 1983, Marji *et al.* 2006). It has been shown that the higher order displacement discontinuity method gives an accurate solution of normal displacement discontinuity (crack opening displacement) and shear displacement discontinuity (crack sliding displacement) near the crack ends (Marji *et al.* 2006, 2009).

The Mode I and Mode II stress intensity factors (SIFs) can be formulated based on these discontinuities using the Linear Elastic Fracture Mechanics (LEFM) principles (Irwin 1957). In this method, special crack tip elements can be used to account for the singularities in the stress and displacement fields near the crack tips. This method also eliminates the need for boundary meshes (elements) as the two sides of the line cracks are simultaneously discretized with similar boundary conditions.

5.1 Higher order displacement discontinuity method (HODDM)

The displacement discontinuities along the boundary of the problem can be achieved more accurately by using higher

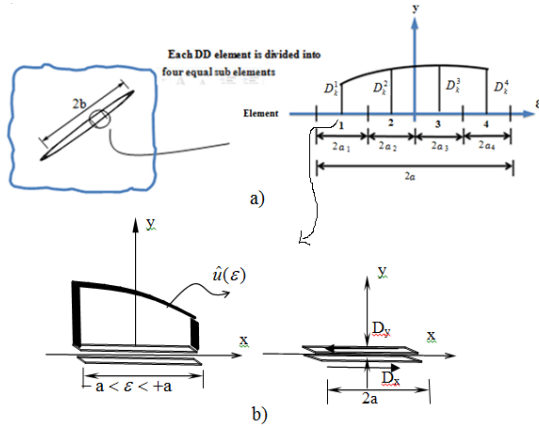


Fig. 5(a) Cubic collocations for the DD variation, (b) the widespread displacement discontinuity variable $u(\epsilon)$ and Constant element displacement discontinuity

order displacement discontinuity (HODD) elements (e.g., quadratic or cubic HODD elements) in the solution of cracked elastostatic bodies. This method is basically a special version of the dual BEM originally proposed by Hong and Chen (1998a), (1998b), and Chen and Hong (1999).

In the present method, a cubic (DD) element ($D_k(\epsilon)$) is divided into four equal sub-elements and each sub-element contains a central node for which the nodal displacement discontinuity (DD) is evaluated numerically (the opening displacement discontinuity D_y and sliding displacement discontinuity D_x) (Fig. 5(a)).

$$D_k(\epsilon) = \sum_{i=1}^4 \Pi_i(\epsilon) D_k^i, \quad k = x, y, \quad i = 1, 2, 3, 4 \quad (2)$$

$$D_x(\epsilon) = \Pi_1(\epsilon) D_x^1 + \Pi_2(\epsilon) D_x^2 + \Pi_3(\epsilon) D_x^3 + \Pi_4(\epsilon) D_x^4$$

$$D_y(\epsilon) = \Pi_1(\epsilon) D_y^1 + \Pi_2(\epsilon) D_y^2 + \Pi_3(\epsilon) D_y^3 + \Pi_4(\epsilon) D_y^4$$

Where D_k^1 (i.e. D_x^1 and D_y^1), D_k^2 (i.e. D_x^2 and D_y^2), D_k^3 (i.e. D_x^3 and D_y^3) and D_k^4 (i.e. D_x^4 and D_y^4) are the cubic nodal displacement discontinuities.

D_x and D_y can be calculated by taking the u_x and u_y components of the widespread displacement discontinuity $u(\epsilon)$, in the interval $(-a, +a)$ as shown in Fig. 5(b), two DD element surfaces can be recognized, one on the positive side of y ($y=0_+$) and the other on the negative side ($y=0_-$). Therefore the fundamental variables D_x and D_y can be written as (Marji *et al.* 2007)

$$D_x = u_x(x, 0_-) - u_x(x, 0_+), \quad (2)$$

$$D_y = u_y(x, 0_-) - u_y(x, 0_+)$$

and,

$$\begin{aligned} \Pi_1(\epsilon) &= -(3a_1^3 - a_1^2\epsilon - 3a_1\epsilon^2 + \epsilon^3)/(48a_1^3), \\ \Pi_2(\epsilon) &= (9a_1^3 - 9a_1^2\epsilon - a_1\epsilon^2 - \epsilon^3)/(16a_1^3), \\ \Pi_3(\epsilon) &= (9a_1^3 + 9a_1^2\epsilon - a_1\epsilon^2 - \epsilon^3)/(16a_1^3), \\ \Pi_4(\epsilon) &= -(3a_1^3 + a_1^2\epsilon - 3a_1\epsilon^2 - \epsilon^3)/(48a_1^3) \end{aligned} \quad (3)$$

are the cubic collocation shape functions using $a_1=a_2=a_3=a_4$. A cubic element has 4 nodes, which are the centers of its four

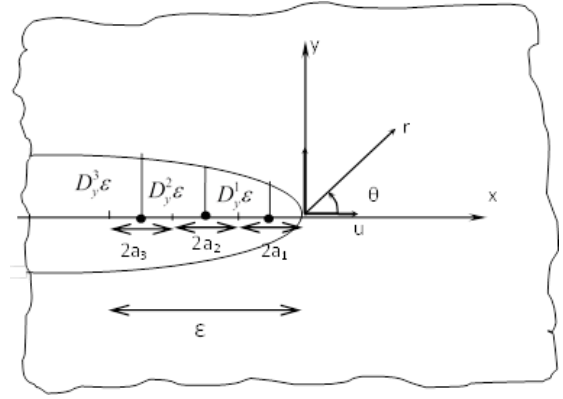


Fig. 6 A special crack tip element with three equal sub-elements

sub-elements as shown in Fig.

Since stress and displacement singularities at the crack ends may reduce the computational accuracy, special crack tip elements are used to increase the accuracy of the DDs near the crack tips (Marji *et al.* 2006). As shown in Fig. 6, the DD variation for three nodes can be formulated using a special crack tip element containing three nodes (or having three special crack tip sub-elements).

$$D_k(\epsilon) = [\Gamma_{C1}(\epsilon)]D_k^1(a) + [\Gamma_{C2}(\epsilon)]D_k^2(a) + [\Gamma_{C3}(\epsilon)]D_k^3(a), \quad k = x, y \quad (4)$$

where, the crack tip element has a length $a_1=a_2=a_3$.

Considering a crack tip element with the three equal sub-elements ($a_1=a_2=a_3$), the shape functions $\Gamma_{C1}(\epsilon)$, $\Gamma_{C2}(\epsilon)$, and $\Gamma_{C3}(\epsilon)$ can be written as

$$\begin{aligned} \Gamma_{C1}(\epsilon) &= \frac{15\epsilon^2}{8a_1^2} - \frac{\epsilon^2}{a_1^2} + \frac{\epsilon^2}{8a_1^2}, \\ \Gamma_{C2}(\epsilon) &= \frac{-5\epsilon^2}{8a_1^2} + \frac{3\epsilon^2}{2\sqrt{3}a_1^2} - \frac{\epsilon^2}{4\sqrt{3}a_1^2}, \\ \Gamma_{C3}(\epsilon) &= \frac{3\epsilon^2}{8\sqrt{5}a_1^2} - \frac{\epsilon^2}{2\sqrt{5}a_1^2} + \frac{\delta^2}{8\sqrt{5}a_1^2} \end{aligned} \quad (5)$$

Considering a body of arbitrary shape with a crack of arbitrary size, subjected to arbitrary tensile and shear loadings (i.e., the mixed mode loading I and II), the details of the derivation of stresses and displacements near the crack tip can find in the related text books (Crouch and Starfield 1983, Aliabadi 1998). For the displacement discontinuity method used here, the following formulations are suitable

$$\begin{aligned} \sigma_x &= \frac{K_I}{\sqrt{2\pi r}} \cos \frac{\theta}{2} (1 - \sin \frac{\theta}{2} \sin \frac{3\theta}{2}) - \frac{K_{II}}{\sqrt{2\pi r}} \sin \frac{\theta}{2} (2 + \cos \frac{\theta}{2} \cos \frac{3\theta}{2}) \\ \sigma_y &= \frac{K_I}{\sqrt{2\pi r}} \cos \frac{\theta}{2} (1 + \sin \frac{\theta}{2} \sin \frac{3\theta}{2}) + \frac{K_{II}}{\sqrt{2\pi r}} \sin \frac{\theta}{2} \cos \frac{\theta}{2} \cos \frac{3\theta}{2} \\ \sigma_{xy} &= \frac{K_I}{\sqrt{2\pi r}} \cos \frac{\theta}{2} \sin \frac{\theta}{2} \cos \frac{3\theta}{2} + \frac{K_{II}}{\sqrt{2\pi r}} \cos \frac{\theta}{2} (1 - \sin \frac{\theta}{2} \sin \frac{3\theta}{2}) \end{aligned} \quad (6)$$

Where, K_I and K_{II} are the stress intensity factors in mode

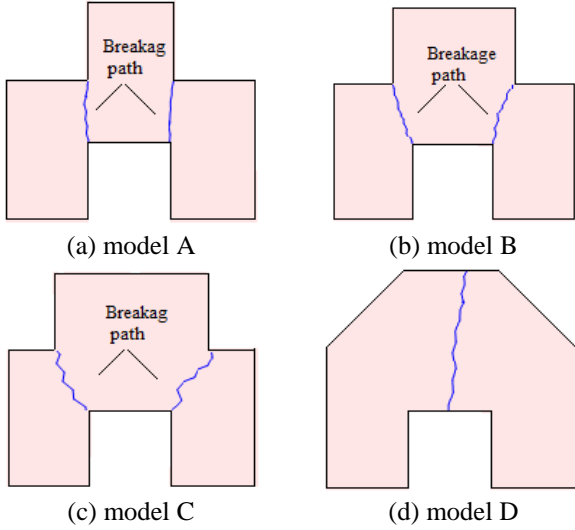


Fig. 7 Numerical simulation of crack propagation paths for the concrete specimens with different geometry models (a) model A (b) model B; (c) model C; (d) model D

I mode II respectively; $\mu = E/[2(1+\nu)]$ is the shear modulus; E is young's modulus; ν is Poisson's ratio of the brittle material; $\lambda=(3-4\nu)$ for plane strain condition; and $\lambda=(3-\nu)/(1+\nu)$ for plane stress condition and r and θ are defined in Fig. 6.

$$u = \frac{1}{4\mu} \sqrt{\frac{r}{2\pi}} \begin{bmatrix} K_I \left((2k-1) \cos \frac{\theta}{2} - \cos \frac{3\theta}{2} \right) + \\ K_{II} \left(-(2k-1) \sin \frac{\theta}{2} + 3 \sin \frac{3\theta}{2} \right) \end{bmatrix} \quad (7)$$

$$v = \frac{1}{4\mu} \sqrt{\frac{r}{2\pi}} \begin{bmatrix} K_I \left(-(2k+1) \sin \frac{\theta}{2} + \sin \frac{3\theta}{2} \right) + \\ K_{II} \left(-(2k+1) \cos \frac{\theta}{2} + 3 \cos \frac{3\theta}{2} \right) \end{bmatrix}$$

$$u(\theta = \pi) - u(\theta = -\pi) = \frac{k+1}{\mu} K_I \sqrt{\frac{r}{2\pi}} \quad (8)$$

$$v(\theta = \pi) - v(\theta = -\pi) = \frac{k+1}{\mu} K_{II} \sqrt{\frac{r}{2\pi}}$$

Based on the linear elastic fracture mechanics (LEFM) principles, the Mode I and Mode II stress intensity factors K_I and K_{II} , (expressed in MPa m^{1/2}) can be written in terms of the normal and shear displacement discontinuities obtained for the last special crack tip element as (Shou and Crouch 1995)

$$K_I = \frac{\mu}{4(1-\nu)} \left(\frac{2\pi}{a_1} \right)^{\frac{1}{2}} D_y(a_1), \quad \text{and} \quad (9)$$

$$K_{II} = \frac{\mu}{4(1-\nu)} \left(\frac{2\pi}{a_1} \right)^{\frac{1}{2}} D_x(a_1)$$

where μ is the shear modulus and ν is Poisson's ratio of the brittle material.

5.2 Numerical simulations

Because of the symmetry in the specimens, loading, and the observed fracture pattern, the numerical simulations were done in 2D using a two-dimensional higher order displacement discontinuity method explained above. This numerical analysis is based on the two dimensional plain strain conditions, commonly used for numerical simulations.

Cubic elements formulation of displacement discontinuities along with three special crack tip elements is used. A cubic distribution of displacement discontinuities is assumed along each boundary element with only two degrees of freedom. Although using three special elements for the treatment of each crack tip is somewhat complicated but it will highly increase the accuracy of the displacement discontinuity variations near these singular ends.

The Linear Elastic Fracture Mechanics (LEFM) theory is used to calculate the stress intensity factors (SIFs) and σ -criterion is also implemented in the computer code to predict the possibility of shear crack propagation path.

The crack propagation paths are estimated by using a standard iterative. In the present analyses, to investigate the crack propagation and shear phenomenon, the concrete specimens are studied under compression loading. The crack propagation path has been estimated by the proposed method. In this iterative method, the cubic displacement discontinuity elements give accurate results for the Mode I and Mode II stress intensity factors.

The same concrete specimens (studied experimentally in section 4) are also numerically modeled by the modified HODDM code. The HODDM code has the potential of predicting the shear cracks and specimen breakage due to crack propagation.

The concrete specimens (shown in Figs. 4(a)-(d)) were modeled by the indirect boundary element method and the crack propagation paths are graphically shown in Figs. 7(a)-(d). In the present numerical simulations, the Mode I and Mode II stress intensity factors (SIFs) proposed by Irwin (1957) are estimated based on LEFM approach. A boundary element code is provided using the maximum tangential stress criterion given by Erdogan and Sih (1963) in a stepwise procedure to predict the propagation paths for the wing cracks. As shown in Figs. 7(a)-(d), the simulated fracture paths are in good agreements with the corresponding experimental results.

6. Conclusions

The mechanism of crack propagation in concrete specimens under shear loading has been studied by a coupled experimental and numerical approach.

Shear tests were conducted on concrete specimens with four different geometries. These specimens were subjected to compressional load and failed under indirect shear loading condition. The experimental results were analyzed to evaluate the shear behavior of concrete specimens with different geometries. It has been shown that the shear fracturing of specimens occur mainly by the propagation of wing cracks emanating from the edges of the specimen.

The modified higher order displacement discontinuity code (HDDM code) was employed to simulate the experimental results and specially the fracturing pattern in the specimens. The numerical models captured well the shear behavior of the specimen and the cracks propagation paths. The proposed method can be used in a vast variety of geomechanical projects in various engineering and bioengineering fields dealing with fracturing of solids and porous materials in continuum and discontinuous mechanics.

It can be concluded that in models A, B and C, the cracks are initiated from the edges of specimens, but for model D, the cracks are not initiated from the edges and the specimen is failed due to the appearance of a single fracturing surface.

In this study, it has been shown that there is a good agreement between the corresponding numerical and experimental results which enables one to clearly understand the fracturing mechanism of concrete specimens. The experiments and numerical simulations carried out in this study can contribute to a safer design of concrete structures.

References

- ACI Committee 544 (2008), *Report on Fiber Reinforced Concrete*.
- Aliabadi, M.H. (1998), *Fracture of Rocks*, Computational Mechanics Publications, Southampton, U.K.
- ASTM International C 1018-97 (2002), *Standard Test Method for Flexural Toughness and First-Crack Strength of Fiber-Reinforced Concrete (Using Beam With Third-Point Loading)*, **4**(2), 546-553.
- Ayatollahi, M.R. and Aliha, M.R. (2008), "On the use of Brazilian disc specimen for calculating mixed mode I-II fracture toughness of rock materials", *Eng. Fract. Mech.*, **75**(16), 4631-4641.
- Ayatollahi, M.R. and Sistaninia, M. (2011), "Mode II fracture study of rocks using Brazilian disk specimens", *J. Rock Mech. Min. Sci.*, **48**(5), 819-826.
- Barragán, B., Gettu, R., Agullo, L. and Zerbino, R. (2006), "Shear failure of steel fiber-reinforced concrete based on push-off tests", *ACI Mater. J.*, **103**(4), 251-257.
- Bazant, Z.P. and Oh, B.H. (1983), "Crack band theory for fracture of concrete", *Mater. Struct.*, **16**(3), 155-177.
- Chen, J.T. and Hong, H.K. (1999), "Review of dual boundary element methods with emphasis on hyper singular integrals and divergent series", *Appl. Mech. Rev.*, **52**, 17-33.
- Chuang, T. and Mai, Y.W. (1998), "Flexural behavior of strain-softening solids", *J. Sol. Struct.*, **25**, 1427-1443.
- Crouch, S.L. (1967a), *Analysis of Stresses and Displacements around Underground Excavations: An Application of the Displacement Discontinuity Method*, University of Minnesota Geomechanics Report, Minneapolis, Minnesota, U.S.A.
- Crouch, S.L. and Starfield, A.M. (1983), *Boundary Element Methods in Solid Mechanics*, Allen and Unwin, London, U.K.
- Dai, F., Chen, R., Iqbal, M.J. and Xia, K. (2010), "Dynamic cracked chevron notched Brazilian disc method for measuring rock fracture parameters", *J. Rock Mech. Min. Sci.*, **47**(4), 606-613.
- Dai, F., Xia, K., Zheng, H. and Wang, Y.X. (2011), "Determination of dynamic rock mode-I fracture parameters using cracked chevron notched semi-circular bend specimen", *Eng. Fract. Mech.*, **78**(15), 2633-2644.
- Deokar, A.A.V. and Wakchaure, B.V.D. (2011), *Experimental Investigation of Crack Detection in Cantilever Beam Using Natural Frequency as Basic Criterion*, Institute of technology, Nirma University, Ahmedabad, India.
- Erdogan, F. and Sih, G.C. (1963), "On the crack extension in plates under loading and transverse shear", *J. Basic Eng.*, **85**(4), 519-527.
- Fortino, S. and Bilotta, A. (2004), "Evaluation of the amount of crack growth in 2D LFM problems", *Eng. Fract. Mech.*, **71**(9), 1403-1419.
- Gehle, C.K. and Kutter, H. (2003), "Breakage and shear behavior of intermittent rock joints", *J. Rock Mech. Min. Sci.*, **40**, 687-700.
- Gerges, N., Issa, C. and Fawaz, S. (2015), "Effect of construction joints on the splitting tensile strength of concrete", *Case Stud. Constr. Mater.*, **3**, 83-91.
- Haeri, H. (2015), "Influence of the inclined edge notches on the shear-fracture behavior in edge-notched beam specimens", *Comput. Concrete*, **16**(4), 605-623.
- Haeri, H. and Sarfarazi, V. (2016a), "The effect of micro pore on the characteristics of crack tip plastic zone in concrete", *Comput. Concrete*, **17**(1), 107-112.
- Haeri, H. and Sarfarazi, V. (2016b), "The effect of non-persistent joints on sliding direction of rock slopes", *Comput. Concrete*, **17**(6), 723-737.
- Haeri, H. and Sarfarazi, V. (2016c), "The deformable multilaminate for predicting the elasto-plastic behavior of rocks", *Comput. Concrete*, **18**(2), 201-214.
- Haeri, H., Sarfarazi, V. and Lazemi, H.A. (2016d), "Experimental study of shear behavior of planar non-persistent joint", *Comput. Concrete*, **17**(5), 639-653.
- Hillerborg, A. (1980), "Analysis of fracture by means of the fictitious crack model, particularly for fiber reinforced concrete", *J. Cement Compos.*, **2**(4), 177-190.
- Hong, H.K. and Chen, J.T. (1988b), "Derivation of integral equations of elasticity", *J. Eng. Mech.*, **114**(6), 1028-1044.
- Irwin, G.R. (1957), "Analysis of stress and strains near the end of a crack", *J. Appl. Mech.*, **24**(3), 361-364.
- Jenq, Y.S. and Shah, S.P. (1985), "Two parameter fracture model for concrete", *J. Eng. Mech.*, **111**(10), 1227-1241.
- Kaplan, M.F. (1961), "Crack propagation and the fracture of concrete", *ACI J.*, **58**(11), 591-610.
- Marji, M.F., Hosseini-nasab, H. and Hossein-morshedy, A. (2009), "Numerical modeling of the mechanism of crack propagation in rocks under TBM disc cutters", *J. Mech. Mater. Struct.*, **2**, 439-457.
- Marji, M.F., Hosseini-nasab, H. and Kohsar, A.H. (2006), "On the uses of special crack tip elements in numerical rock fracture mechanics", *J. Sol. Struct.*, **43**(1), 669-1692.
- Marji, M.F., Hosseini-nasab, H. and Kohsary, A.H. (2007), "A new cubic element formulation of the displacement discontinuity method using three special crack tip elements for crack analysis", *J. Sol. Struct.*, **43**, 61-91.
- Mirsayah, A. and Banthia, N. (2002), "Shear strength of steel fiber-reinforced concrete", *ACI Mater. J.*, **99**(5), 473-479.
- Munikrishna, A. (2008), "Shear behavior of concrete beams reinforced with high performance steel shear reinforcement", M.S. Dissertation, North Carolina State University, U.S.A.
- Nilson, A.H., Darwin, D. and Dolan, C.W. (2004), *Design of Concrete Structures*, 13th Edition, McGraw Hill, New York, U.S.A.
- Ning, J., Liu, X., Tan, Y., Wang, J. and Tian, C. (2015), "Relationship of box counting of fractured rock mass with hoek-brown parameters using particle flow simulation", *Geomech. Eng.*, **9**(5), 619-629.
- Ozcebe, G. (2011), "Minimum flexural reinforcement for T-beams made of higher strength concrete", *Can. J. Civil Eng.*, **26**(5),

- 525-534.
- Panaghi, K., Golshani, A. and Takemura, T. (2015), "Rock failure assessment based on crack density and anisotropy index variations during triaxial loading tests", *Geomech. Eng.*, **9**(6), 793-813.
- Ruiz, G. and Carmona, R.J. (2006a), "Experimental study on the influence of the shape of the cross-section and the rebar arrangement on the fracture of LRC beams", *Mater. Struct.*, **39**(3), 343-352.
- Ruiz, G., Carmona, J.R. and Cendon, D.A. (2006b), "Propagation of a cohesive crack through adherent reinforcement layers", *Comput. Meth. Appl. Mech. Eng.*, **195**(52), 7237-7248.
- Sardemir, M. (2016), "Empirical modeling of flexural and splitting tensile strengths of concrete containing fly ash by GEP", *Comput. Concrete*, **17**(4), 489-498.
- Sarfarazi, V. and Haeri, H. (2016a), "The effect of non-persistent joints on sliding direction of rock slopes", *Comput. Concrete*, **17**(6), 723-737.
- Sarfarazi, V., Faridi, H.R., Haeri, H. and Schubert, W. (2016b), "A new approach for measurement of anisotropic tensile strength of concrete", *Adv. Concrete Constr.*, **3**(4), 269-284.
- Savilahti, T., Nordlund, E. and Stephansson, O. (1990), "Shear box testing and modeling of joint bridge", *Proceedings of the International Symposium on Shear Box Testing and Modeling of Joint Bridge Rock Joints*, Norway.
- Shou, K.J. and Crouch, S.L.A. (1995), "Higher order displacement discontinuity method for analysis of crack problems", *J. Rock Mech. Min. Sci. Geomech. Abstr.*, **32**(1), 49-55.
- Sun, S. and Kuchma, D.A. (2007), *Shear Behavior and Capacity of Large-Scale Prestressed High-Strength Concrete Bulb-Tee Girders*, NSEL Report Series Report No. NSEL-002.
- Tang, H.D. (2015), *Mechanical Behavior of 3D Crack Growth in Transparent Rock-Like Material Containing Preexisting Flaws under Compression*, 1-10.
- Wang, Q.Z. (2010), "Formula for calculating the critical stress intensity factor in rock fracture toughness tests using cracked chevron notched Brazilian disc (CCNBD) specimens", *J. Rock Mech. Min. Sci.*, **47**(6), 1006-1011.
- Weihua, Z., Runqiu, H. and Ming, Y. (2015), "Mechanical and fracture behavior of rock mass with parallel concentrated joints with different dip angle and number based on PFC simulation", *Geomech. Eng.*, **8**(6), 757-767.
- Wong, R.H.C., Leung, W.L. and Wang, S.W. (2001), *Shear Strength Study on Rock-Like Models Containing Arrayed Open Joints*, Swets & ZeitlingerLisse, Leiden, 843-849.
- Wu, Z.M., Yang, S.T., Hu, X.Z. and Zheng, J.J. (2006), "An analytical model to predict the effective fracture toughness of concrete for three-point bending notched beams", *Eng. Fract. Mech.*, **73**(15), 2166-2191.
- Xiang, F., Kulailake, P.H.S.W., Xin, C. and Ping, C. (2015), "Crack initiation stress and strain of jointed rock containing multi-cracks under uniaxial compressive loading: A particle flow code approach", *J. Centr. South Univ.*, **22**(2), 638-645.
- Xu, S.L. and Reinhardt, H.W. (2000), "A simplified method for determining double-K fracture parameters for three-point bending tests", *J. Fract.*, **104**(2), 181-209.
- Yang, S.Q. (2015), "An experimental study on fracture coalescence characteristics of brittle sandstone specimens combined various flaws", *Geomech. Eng.*, **8**(4), 541-557.
- Yang, S.T., Hu, X.Z. and Wu, Z.M. (2011), "Influence of local fracture energy distribution on maximum fracture load of three-point-bending notched concrete beams", *Eng. Fract. Mech.*, **78**(18), 3289-3299.
- Zhang, X. and Wong, L.N.Y. (2012), "Cracking process in rock-like material containing a single flaw under uniaxial compression: A numerical study based on parallel bonded-particle model approach", *Rock Mech. Rock Eng.*, **45**(5), 711-737.
- Zhang, X. and Wong, R.H.C. (2013), "Crack initiation, propagation and coalescence in rock-like material containing two flaws: A numerical study based on bonded-particle model approach", *Rock Mech. Rock Eng.*, **46**(5), 1001-1021.
- Zhao, C. (2015), "Analytical solutions for crack initiation on floor-strata interface during mining", *Geomech. Eng.*, **8**(2), 237-255.

CC